Available online at www.sciencedirect.com
ScienceDirect
Remote Sensing of Environment 107 (2007) 194–199
Remote Sensing of Environment
www.elsevier.com/locate/rse

Cloud motion vectors from MISR using sub-pixel enhancements

Roger Davies [a,*], Ákos Horváth [b], Catherine Moroney [c], Banglin Zhang [d], Yanqiu Zhu [d]

[a] Department of Physics, The University of Auckland, New Zealand
[b] Rosenstiel School of Marine and Atmospheric Science, University of Miami, FL, USA
[c] Jet Propulsion Laboratory, California Institute of Technology, Pasadena, CA, USA
[d] Global Modeling and Assimilation Office, NASA Goddard Space Flight Center, Greenbelt, MD USA

Received 23 May 2006; received in revised form 27 August 2006; accepted 12 September 2006

Abstract

The operational retrieval of height-resolved cloud motion vectors by the Multiangle Imaging SpectroRadiometer on the Terra satellite has been significantly improved by using sub-pixel approaches to co-registration and disparity assessment, and by imposing stronger quality control based on the agreement between independent forward and aft triplet retrievals. Analysis of the fore-aft differences indicates that CMVs pass the basic operational quality control 67% of the time, with rms differences — in speed of 2.4 m/s, in direction of 17°, and in height assignment of 290 m. The use of enhanced quality control thresholds reduces these rms values to 1.5 m/s, 14° and 165 m, respectively, at the cost of reduced coverage to 45%. Use of the enhanced thresholds also eliminates a tendency for the rms differences to increase with height. Comparison of CMVs from an earlier operational version that had slightly weaker quality control, with 6-hour forecast winds from the Global Modeling and Assimilation Office yielded very low bias values and an rms vector difference that ranged from 5 m/s for low clouds to 10 m/s for high clouds.

Keywords: Cloud motion vector; Atmospheric motion vector; Multi-angle remote sensing; Height-resolved wind; Geometric cloud height; Stereo matching; Wind remote sensing

1. Introduction

Previously (Horváth & Davies, 2001a,b; Moroney et al., 2002), we have reported on the retrieval of cloud motion vectors (CMVs) obtained by the Multiangle Imaging SpectroRadiometer (MISR) on the Terra satellite. These are derived by matching cloud reflectivity patterns from three different view angles (An, B, and D cameras, corresponding to view angles of 0°, 45° and 70°), one pair at a time (i.e., An–B and B–D). The across-track and along-track disparities enter two time-dependent equations that are then solved simultaneously to separate the height and motion effects. This yields the cloud motion components parallel to and orthogonal to the satellite's direction, as well as the height of the cloud top. The retrieval is relatively noisy, and must be repeated many times over a mesoscale domain (of dimension 70.4 km) to obtain a consensus motion vector from the distribution of individual retrievals performed at the 275 m pixel level. Experience with the original operational algorithm showed that it was capable of achieving a theoretical accuracy of ~4 m/s, with a height resolution of ~400 m, for many mesoscale regions, but that higher errors were also common due to limited quality control. In particular, the retrievals were found to be highly sensitive to the precision to which the multiangle views were co-registered to a common reference level.

Accordingly, several improvements have since been made to the original algorithm. As described below, these improvements have led to more accurate, and far more reliable, CMVs. The off-nadir views are now rigorously co-registered to the nadir view with a sub-pixel accuracy of ~0.2 pixels, separately for each orbit, using an automated matching procedure that recognizes land-surface features or sea-ice patterns (Jovanovic et al., 2007 — this issue). Previously, the Da camera (aft view of 70°) had a higher uncertainty in its co-registration, preventing the reliable use of the aft triplet (An–Ba–Da). With the improved co-registration of all cameras, we can now use the Da camera with confidence, and thus obtain two equivalent estimates of the mesoscale CMV, one from the forward triplet (An–Bf–Df), and one from the aft triplet, with their agreement

* Corresponding author.
E-mail address: r.davies@auckland.ac.nz (R. Davies).

0034-4257/$ - see front matter © 2007 Elsevier Inc. All rights reserved.
doi:10.1016/j.rse.2006.09.023

providing a strong measure of quality control. In addition, the distribution of 275-m retrievals is now being interpolated at the sub-pixel level to further improve the precision of the consensus mesoscale vector.

These improvements are described below, followed by an assessment of the new CMV accuracy and results from a comparative study conducted by the Global Modeling and Assimilation Office (GMAO).

2. Retrieval sensitivities to co-registration errors

In Horváth and Davies (2001a) we introduced a simplified model of the wind[1] retrieval problem, in which we ignored the cross-track component of look-vectors and cloud motion, and assumed a non-rotating spherical Earth and circular orbit. This elementary model takes advantage of the fact that the stereo effect is much stronger in the along-track direction than in the cross-track direction and proves helpful in investigating the sensitivity of the retrieval algorithm, at least to along-track camera misregistration. From Eq. (3) in Horváth and Davies (2001a) we can derive an estimate for the sensitivity of the retrieved along-track wind, v_l, and cloud height, h, to the along-track image location in the D and B cameras, x_D, and x_B, respectively. As an example, let us consider the default aftward wind retrieval camera triplet (Da–Ba–An), for which these sensitivities are as follows:

$$\frac{\partial v_l}{\partial x_{\mathrm{Da}}} = \frac{d_1}{t_2 d_1 - t_1 d_2}, \tag{1}$$

$$\frac{\partial v_l}{\partial x_{\mathrm{Ba}}} = -\frac{d_1 + d_2}{t_2 d_1 - t_1 d_2}, \tag{2}$$

$$\frac{\partial h}{\partial x_{\mathrm{Da}}} = -\frac{t_1}{t_2 d_1 - t_1 d_2}, \tag{3}$$

and

$$\frac{\partial h}{\partial x_{\mathrm{Ba}}} = \frac{t_1 + t_2}{t_2 d_1 - t_1 d_2}. \tag{4}$$

(Similar expressions can be obtained for the forward Df and Bf cameras but with opposite sign.) In the above equations, $t_1 = t_{\mathrm{Ba}} - t_{\mathrm{An}}$, $t_2 = t_{\mathrm{Da}} - t_{\mathrm{Ba}}$, $d_1 = \tan\theta_{\mathrm{An}} - \tan\theta_{\mathrm{Ba}}$, and $d_2 = \tan\theta_{\mathrm{Ba}} - \tan\theta_{\mathrm{Da}}$, where t_{An}, t_{Ba}, and t_{Da} are the An, Ba, and Da camera imaging times, and θ_{An}, θ_{Ba}, and θ_{Da} are the An, Ba, and Da camera view angles. In order for the along-track wind to have a positive meridional component, its sign convention treats it as negative if it is in the same direction as the satellite motion down-track. Retrieval uncertainties resulting from an along-track co-registration uncertainty of 1 pixel (275 m) calculated from Eqs. (1), (2), (3), (4) using nominal values for camera view angles and imaging times are summarized in Table 1. This shows that the retrieval uncertainty is 2–3 times more sensitive to B camera co-registration error than it is to D camera co-registration error. This is because the B image location affects both the B–D and the B–An disparities, whereas the D image location affects only the B–D disparity.

Table 1
Retrieval uncertainty in along-track wind, v_l, and cloud height, h, due to a 1-pixel uncertainty ($\Delta x = 275$ m) in Da or Ba along-track co-registration as determined from the simplified model

	Da	Ba
$\frac{\partial v_l}{\partial x}\Delta x$	−5.7 m/s/pixel	15.6 m/s/pixel
$\frac{\partial h}{\partial x}\Delta x$	507 m/pixel	−1132 m/pixel

The simplified model above considers the along-track direction only. In reality, the look-vectors also have cross-track (y-axis) components that introduce a weak coupling between the along-track and cross-track wind retrievals for the general case. Consequently, a co-registration error in the along-track direction creates an error in the cross-track wind as well. Similarly, a co-registration error in the cross-track direction also has an effect on the along-track wind, although this effect is relatively small. In order to get a full picture of the various retrieval uncertainties, we performed a sensitivity analysis with the operational CMV algorithm that treats the 3D nature of the problem properly using ray-intersection. We applied co-registration errors of up to 1 pixel in the along-track and the cross-track directions and show the resulting retrieval errors separately for the Da and Ba cameras in Fig. 1. Retrieval uncertainties corresponding to an along-track or cross-track co-registration uncertainty of 1 pixel are also summarized in Tables 2 and 3, respectively. Comparison of Tables 1–3 shows the following. First, the simplified model is perfectly adequate for estimating retrieval errors due to along-track misregistration. Second, retrievals are more sensitive to along-track misregistration than to cross-track misregistration. In fact, the effects of the latter might be neglected. Finally, the along-track wind is generally more sensitive to misregistration than is the cross-track wind.

The significance of the above findings is that in Horváth and Davies (2001a) we only considered retrieval errors due to finite pixel size. Such random quantization errors, however, tend to cancel out when the mean wind of a mesoscale domain is computed from a few dozen individual retrievals. Systematic errors in camera co-registration, (which tend to persist over large sections of a given orbit), on the other hand, do not cancel out and tend to bias the retrievals. Our current analysis indicates that MISR CMV retrievals are indeed sensitive to misregistration of either the D or B cameras, with the largest retrieval errors occurring for along-track co-registration errors in the B cameras. Although co-registration errors in the B cameras are usually much smaller than in the D cameras, they can still result in significant CMV and height errors due to their enhanced effect on the retrievals. Therefore, we have implemented an algorithm that, in the presence of visible land-surface or sea-ice features, improves not only the D but also the B camera

[1] For ease of readability, the technically correct 'CMV' is often referred to simply as 'wind'.

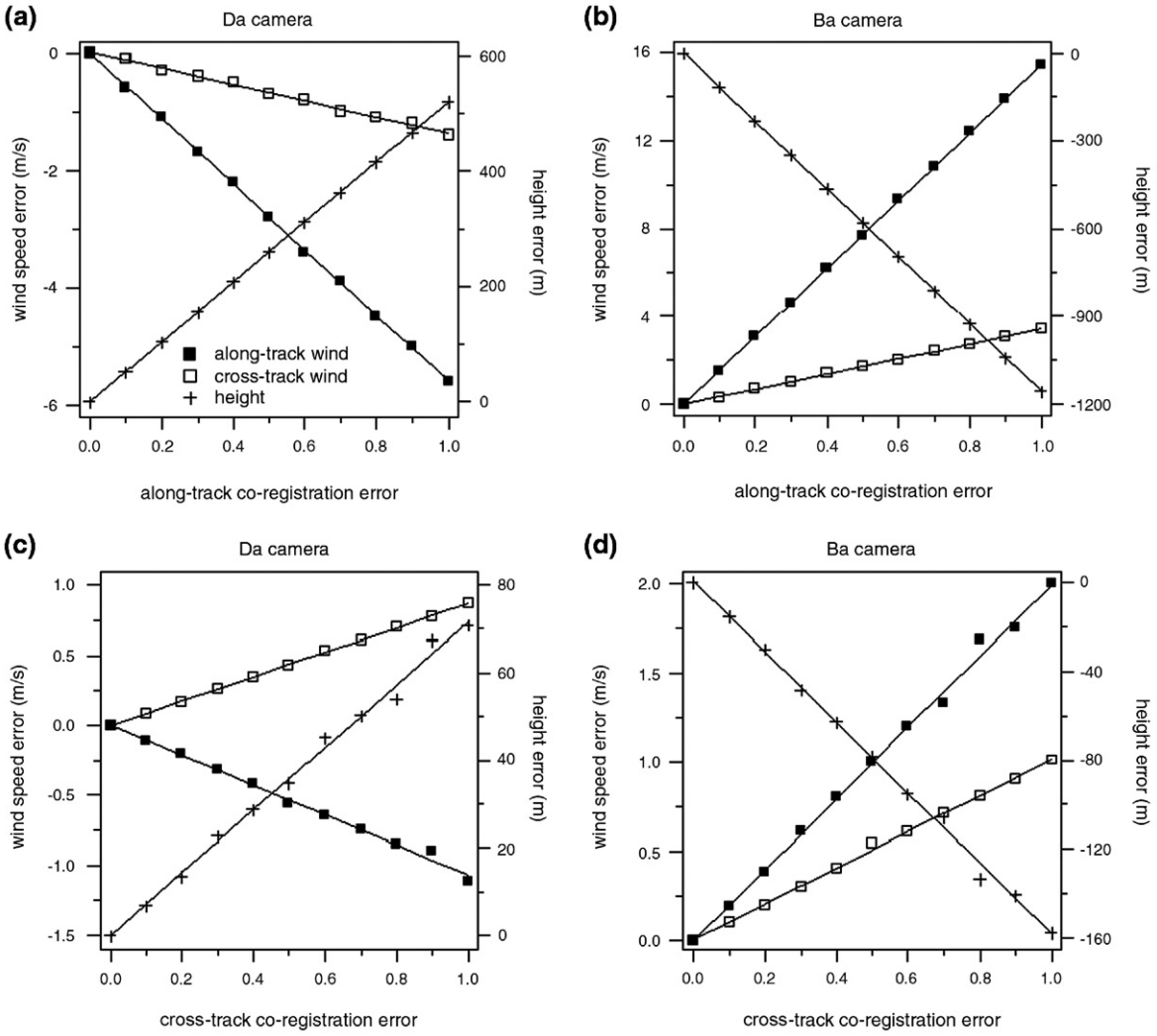

Fig. 1. Retrieval error in along-track wind (solid boxes), cross-track wind (empty boxes), and cloud height (plus signs) versus co-registration error as determined from the operational ray-intersection algorithm: (a) Da along-track misregistration, (b) Ba along-track misregistration, (c) Da cross-track misregistration, and (d) Ba cross-track misregistration. Note that solid lines are linear fits, misregistration is given in 275-m pixels, and the along-track and cross-track winds are positive towards north and east, respectively.

co-registration. This is performed at the sub-pixel level, separately for each orbit (Jovanovic et al., 2007 — this issue).

In addition to these co-registration enhancements, the analysis of the measured disparities has also been improved. Previously, along-track and cross-track disparities retrieved over a given domain were sorted into a 2D histogram, and then the final mesoscale wind was computed from the most populated histogram bin. Because the MISR stereo matchers have no sub-pixel capability, this meant that the modal along-track and cross-track disparities were always quantized as integer values. In the updated algorithm, the final mesoscale wind is calculated as the weighted average of the most

Table 2
Retrieval uncertainty in along-track wind, v_l, cross-track wind, v_c, and cloud height, h, due to a 1-pixel uncertainty (Δx=275 m) in Da or Ba along-track co-registration as determined from the operational ray-intersection algorithm

	Da	Ba
$\frac{\partial v_l}{\partial x}\Delta x$	−5.6 m/s/pixel	15.5 m/s/pixel
$\frac{\partial v_c}{\partial x}\Delta x$	−1.4 m/s/pixel	3.4 m/s/pixel
$\frac{\partial h}{\partial x}\Delta x$	519 m/pixel	−1159 m/pixel

Table 3
Retrieval uncertainty in along-track wind, v_l, cross-track wind, v_c, and cloud height, h, due to a 1-pixel uncertainty (Δy=275 m) in Da or Ba cross-track co-registration as determined from the operational ray-intersection algorithm

	Da	Ba
$\frac{\partial v_l}{\partial y}\Delta y$	−1.1 m/s/pixel	2.0 m/s/pixel
$\frac{\partial v_c}{\partial y}\Delta y$	0.9 m/s/pixel	1.0 m/s/pixel
$\frac{\partial h}{\partial y}\Delta y$	72 m/pixel	−159 m/pixel

Table 4
Quality control thresholds applied to the component differences between mesoscale CMV retrievals obtained separately using forward triplet views (An–Bf–Df) and aft triplets (An–Ba–Da)

	Basic thresholds (all must be satisfied for 'good' winds)	Enhanced thresholds (two or more must be satisfied for 'better' winds)
NS wind component	10 m/s	3 m/s
EW wind component	3 m/s	1 m/s
Height	1000 m	300 m
Direction	45°	Not used

populated bin and the surrounding bins. This yields more precise (floating point) values for the modal disparities, even though the input disparities are still integers. Experience with the new algorithm indicates that the enhanced co-registration and modal disparity computation contribute about equally to reducing the rms errors in the updated CMVs, with the co-registration error being mainly responsible for the bias error.

3. Comparison of forward and aft CMV retrievals

3.1. Quality control

In addition to the above enhancements, a more rigorous quality control has now been implemented. The main quality check is obtained by comparing the forward triplet retrieval with that from the aft triplet. If any one of the fore-aft retrievals of height, CMV direction, or either wind component, differs by a basic threshold, then the quality is labeled 'bad'. Since directionality loses its significance as the wind speed drops to zero, the directionality threshold is applied only to wind speeds >2 m/s. For operational purposes, the basic thresholds are chosen empirically with fairly broad tolerance, with the intention of removing gross blunders due to either co-registration error or stereo mismatches. No attempt is made to further salvage 'bad' CMVs, although this may be possible for special cases that can be studied at greater depth. This yields the basic data set of operationally retrieved 'good' CMVs that are used in the subsequent comparison with the GMAO.

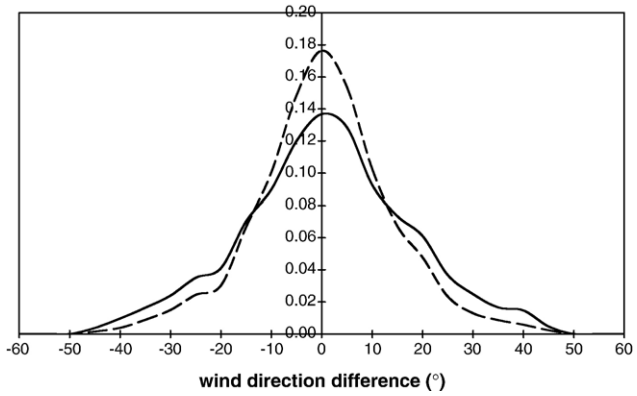

Fig. 3. Frequency distribution of CMV direction differences between the forward and aft triplet retrievals, for cases that satisfy the quality control at a level of 'good' (solid) or 'better' (dashed).

Intended for research, rather than for basic operational purposes, a subset of improved quality, or 'better', CMVs is also obtained from the 'good' CMV data set by setting enhanced thresholds for the height and wind components. For a 'good' CMV to be labeled 'better' it must satisfy at least two of the enhanced thresholds. The basic and enhanced thresholds are summarized in Table 4.

3.2. Analysis of differences

To assess the internal consistency of the CMV retrievals, the forward and aft differences were analyzed over a randomly chosen set of 10 orbits. This produced sufficient data for representative statistics. The frequency distributions of the differences between the forward and aft retrievals are shown in Figs. 2–4 for, respectively, the scalar wind speed, the wind direction, and the wind height. The 'better' distributions are narrower than the 'good' distributions, as expected from their definition, and both distributions are relatively unbiased and symmetric. The shape of the distributions helps to indicate the role of the thresholds, as these cut off the tails of the overall distributions. For most of these, the effect is simply to remove outliers from the tail of the distribution. For the 'better'

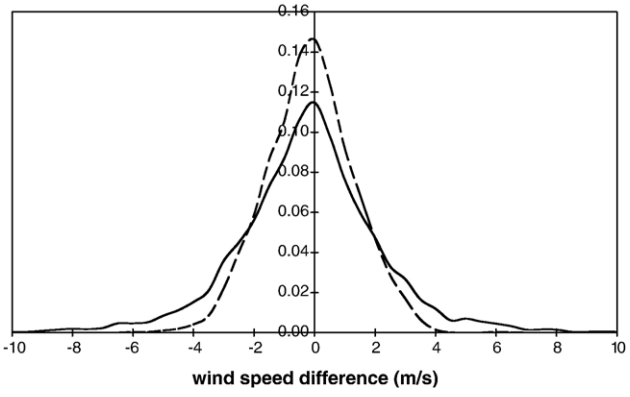

Fig. 2. Frequency distribution of CMV speed differences between the forward and aft triplet retrievals, for cases that satisfy the quality control at a level of 'good' (solid) or 'better' (dashed).

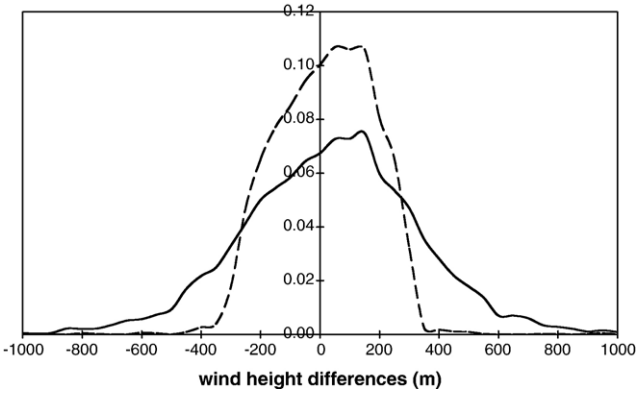

Fig. 4. Frequency distribution of CMV height differences between the forward and aft triplet retrievals, for cases that satisfy the quality control at a level of 'good' (solid) or 'better' (dashed).

Table 5
Summary statistics for the differences between fore and aft CMV retrievals using the current basic and enhanced thresholds, as well as for the earlier basic thresholds used in the GMAO comparison

	All	'Good'	'Better'	'Good' (GMAO)
Number	10,237	6866	4602	6295
Coverage	100%	67%	45%	61%
Speed bias (m/s)	−0.10	−0.20	−0.14	−0.17
Speed rms (m/s)	19.1	2.4	1.5	2.7
Direction bias	3.1°	0.9°	0.5°	2.2°
Direction rms	55°	17°	14°	24°
Vector rms (m/s)	23.2	3.7	2.2	3.9
Height bias (m)	133	38	18	30
Height rms (m)	2102	291	165	649

wind-height differences, the enhanced height difference threshold probably limits the distribution a little too strongly for the rejected data to be called outliers.

The mean and rms of the fore-aft wind-speed, wind-direction, and wind-height differences, together with the vector rms difference, and the overall coverage, are summarized in Table 5. In the absence of a fore-aft quality control, the rms differences are quite high due to the presence of blunders. The low wind-speed bias in the absence of quality control shows simply that the blunders are not preferentially positive or negative. Some of these blunders could be removed by other techniques, as by examining the original disparity histograms, which would eliminate about 10% of the data and reduce the rms speed error to about 13 m/s. However, the fore-aft quality control is far more effective. This quality control comes at the expense of eliminating about one third of the total coverage, but some of this includes clear regions, multi-leveled clouds, and featureless clouds for which the triplet stereo approach is not effective anyway.

The difference between 'good' and 'better', in terms of overall statistics, is not profound. By using the enhanced thresholds, the rms speed difference reduces to 1.5 m/s with a coverage that is still almost half of the data. It would of course be possible to reduce this difference further, eliminating more data, but for the following we simply address the 'good', or operational product.

4. Comparison with the Global Modeling and Assimilation Office

The MISR CMVs were also compared against the 6-hour model forecast winds from version 4.03 of the GEOS data assimilation and forecast systems of the GMAO (GEOS-4). The GEOS-4 is composed of a general circulation model (Suarez & Takacs, 1995) and the physical-space statistical analysis system (PSAS) of Cohn et al. (1998). A 6-week data set starting 1 September 2003 was used for this comparison. The operational MISR product for 'good' winds, version 4.0, included the sub-pixel enhancements mentioned above, but used a slightly earlier version of the quality control, with tighter basic thresholds for the along-track wind difference, and no across-track, height, or direction thresholds. These thresholds are somewhat correlated, so the overall differences in quality are not very great. The summary statistics for the fore-aft differences for the same version of processing used in the comparison set are also given in Table 5. These values are slightly higher than for the current 'good' winds.

The GMAO analyses are a combination of information from the forecast model and several types of observations. The latter include wind and mass profiles from radiosondes, conventional surface observations, aircraft measurements, surface wind data from satellite scatterometers, geostationary satellite AMVs (atmospheric motion vectors that may include both cloud and water vapor features), mass and humidity data from infrared and microwave satellite sounders, and total precipitable water from passive microwave imagers.

The results of this comparison are summarized in Table 6. The bias difference appears to be very low, and is nearly zero for the low-level and mid-level winds. The rms vector difference is ~ 5 m/s for low-level winds, rising with height. While the rms uncertainty in the GMAO forecast winds, which are short-term forecasts issued from GMAO analyses, is not known definitively, the increased rms difference between MISR and GMAO with height was not expected to be as large an effect, since the MISR technique is in principle independent of height. However, on stratifying the fore-aft differences with height for version 4.0 of the operational 'good' winds, these also increased with height, as shown in Fig. 5. Part of the explanation is that the cross-track wind component increases

Table 6
Comparison of MISR wind retrievals with forecast winds from the Global Modeling and Assimilation Office

	Low-level (>700 hPa)	Mid-level (400–700 hPa)	High-level (<400 hPa)
Speed bias (m/s)	0.09	−0.02	1.01
Rms vector difference (m/s)	5.1	7.4	10.5
Mean speed (m/s)	8.6	12.1	24.3
Normalized rms vector difference (m/s)	0.59	0.62	0.43
Number of observations	70,091	12,442	2631

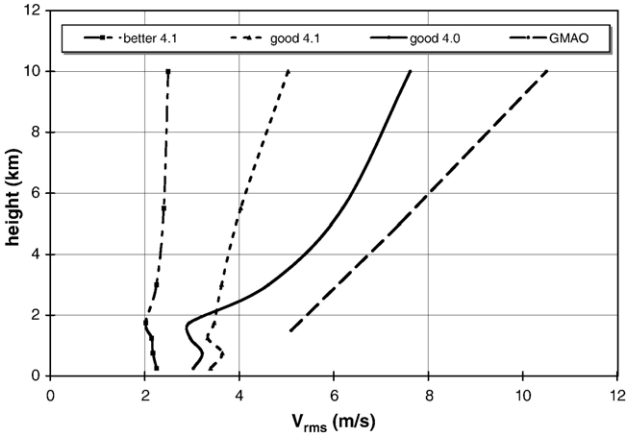

Fig. 5. Vector rms speed differences as a function of height (km). From left to right: 'better' fore-aft differences for version 4.1; 'good' fore-aft differences for version 4.1; 'good' fore-aft differences for version 4.0; differences between MISR 'good' version 4.0 and GMAO forecast winds.

with height, and no quality control on this variable was implemented in version 4.0. In the current version (4.1), most of the height dependence of the vector rms differences disappears, and for the 'better' winds it disappears completely, also shown in Fig. 5. At low levels, which dominate the overall data set due to their greater population, the fore-aft differences in both versions of the 'good' winds indicate a vector rms difference of about 3.5 m/s. Since the difference with the GMAO forecast winds is about 5.1 m/s, there remains about 3.7 m/s of difference (subtracting in quadrature) that is not explained. Some of this may be attributable to the uncertainties related to the height assignment of the MISR winds and in the forecast winds. For upper-level winds, the unexplained difference rises to about 7.2 m/s, albeit for much fewer samples.

5. Discussion

With the implementation of the changes described here, notably the use of sub-pixel co-registration and a fore-aft quality control, the operational MISR wind product has likely reached full maturity. With 67% coverage, the rms speed error is ~ 2.4 m/s, the rms direction error for winds over 2 m/s is ~ 17°, and the rms height error of the CMVs is ~ 300 m. These errors appear to lack measurable bias. Comparison with the GMAO forecast winds over an extensive data set also shows very low bias. The rms vector speed differences with the GMAO rise from ~ 5 to ~ 10 m/s from low to high troposphere. Some of the difference in the upper troposphere is attributable to a weaker quality control in the version of the MISR operational product that was used in the GMAO comparison. This quality control has been strengthened in the current version. Some of the difference remains unexplained, and may be due in part to the higher wind speeds and greater wind shear that exists in the upper troposphere. For these, the height assignment of the CMVs plays a crucial role. By providing a geometrically based height assignment (with known uncertainty), the MISR CMVs are insensitive to assumptions about the atmospheric temperature profile, but the comparison with other techniques, done in pressure coordinates, will introduce some uncertainty.

From the perspective of producing a superior quality product, the 'better' winds quality control yields a wind speed rms of ~ 1.5 m/s with a height uncertainty of ~ 165 m that may be useful for in-depth dynamical case studies.

Future plans include investigating the impact of these winds, especially from data sparse areas, on forecast skill.

Acknowledgements

Part of this research was conducted when R. Davies and Á. Horváth were at the Jet Propulsion Laboratory, under a contract from the National Aeronautics and Space Administration. The MISR data were supplied by the NASA Langley Research Center Atmospheric Science Data Center. D.J. Diner, V. Jovanovic, and L-P. Riishojgaard are thanked for their useful discussions.

References

Cohn, S. E., da Silva, A., Guo, J., Sienkiewicz, M., & Lamich, D. (1998). Assessing the effects of data selection with the DAO physical-space statistical analysis system. *Monthly Weather Review*, *126*, 2913−2926.

Horváth, A., & Davies, R. (2001). Feasibility and error analysis of cloud motion wind extraction from near-simultaneous multiangle MISR measurements. *Journal of Atmospheric and Oceanic Technology*, *18*, 591−608.

Horváth, A., & Davies, R. (2001). Simultaneous retrieval of cloud motion and height from polar-orbiter multiangle measurements. *Geophysical Research Letters*, *28*, 2915−2918.

Jovanovic, V., Moroney, C., & Nelson, D. (2007-this issue). Multi-angle geometric processing for globally geo-located and co-registered MISR image data. *Remote Sensing of Environment*, *107*, 22−32.

Moroney, C., Horváth, A., & Davies, R. (2002). Use of stereo-matching to coregister multiangle data from MISR. *IEEE Transactions on Geoscience and Remote Sensing*, *40*, 1541−1546.

Suarez, M., & Takacs, L. L. (1995). Documentation of the ARIES/GEOS Dynamical Core, Version 2. *NASA Technical Memorandum 104606*, *5*, 45 pp.